SAND-ROSE SHAPED β-$Ni(OH)_2$ MICROSPHERES: A HIGH EFFICIENT ADDITIVE IN THE THERMAL DECOMPOSITION OF AMMONIUM PERCHLORATE

Vesselina Rangelova[1], Maya Spassova[1],
George Tzvetkov[1], Tony Spassov[1], Peter Tzvetkov[2]

[1]*Faculty of Chemistry and Pharmacy, University of Sofia*
J. Bourchier 1, Sofia 1164, Bulgaria
[2]*Institute of General and Inorganic Chemistry*
Bulgarian Academy of Sciences, Sofia 1113, Bulgaria
E-mail: george.tzvetkov@gmail.com; tspassov@ chem.uni-sofia.bg

Received 11 June 2023
Accepted 09 August 2023
DOI: 10.59957/jctm.v59.i1.2024.13

ABSTRACT

Sand-rose shaped β-$Ni(OH)_2$ submicron particles were successfully synthesized by a simple wet-chemistry process. The influence of the as-prepared material on the thermal decomposition of ammonium perchlorate (AP) was explored by thermogravimetry and differential scanning calorimetry analyses. The in-situ formation of active NiO species in the AP/β-$Ni(OH)_2$ system is beneficial for electron transfer in the decomposition steps of AP, leading to the acceleration of its thermal decomposition. In particular, the addition of 5 wt. % β-$Ni(OH)_2$ to AP lowers the decomposition temperature of the latter by 68.5°C and, moreover, the apparent heat of decomposition is increased almost twofold compared to that of pure AP.

Keywords: ammonium perchlorate, $Ni(OH)_2$, NiO, thermal analysis, microstructure.

INTRODUCTION

As a powerful oxidant, ammonium perchlorate (NH_4ClO_4, AP) is the main component of solid rocket propellants [1]. Therefore, the efficiency and burn rate of AP-based fuel formulations strongly depend on the thermal decomposition characteristics of AP. In this regard, numerous studies have shown that nano- and micrometer-sized transition metals and metal oxides can be considered as suitable catalysts for the combustion rate of AP [1]. Recently, Zhai et al. described the preparation of core-shell structured AP/$Co_3(CH_3COO)_5(OH)$ composite [2]. The authors showed that $Co_3(CH_3COO)_5(OH)$ decomposes with increasing temperature, and generates CoO nanoparticles, which have a remarkable catalytic effect on the thermal decomposition of AP. Similar results were reported by Zhang et al. on the influence of nanostructured γ-AlOOH on the thermal behavior of AP [3]. Briefly, γ-AlOOH decomposes, producing renascent γ-Al_2O_3 and α-AlOOH nanoparticles with high catalytic activity. Thus, the use of metal salts and hydroxides can be considered as a promising way to improve the combustion efficiency of AP.

The aim of this work is to demonstrate the performance of newly synthesized sand-rose like β-$Ni(OH)_2$ microspheres as a potential catalytic and energetic additive to improve the thermal decomposition properties of AP. The synthesis protocol employed in this work is based on our recent studies on the Leidenfrost-facilitated hydrolysis of metal ammine complexes [4, 5]. Thus, the β-$Ni(OH)_2$ microstructures have been successfully prepared by a simple, fast and cost-effective method. The physico-chemical properties of the as-prepared material were studied and their effects on the thermal decomposition of AP were thoroughly analyzed.

EXPERIMENTAL

All chemicals used in this investigation were of analytical grade. First, 0.2 g $Ni(CH_3COO)_2.4H_2O$ was dissolved in 2.5 cm^3 25 % NH_3 solution to form $[Ni(NH_3)_6]^{2+}$. Then, the resulting solution was diluted

to 50 cm^3 with water in a beaker. The hydrolysis of the complex to β-$Ni(OH)_2$ was realized at Leidenfrost situation, created by directly placing the vessel for 2 min onto the overheated hot plate (300ºC). The obtained green precipitate was filtered, washed and air-dried for 24 h. In addition, β-$Ni(OH)_2$ sample was characterized by X-ray diffraction (XRD, Bruker D8 Advance diffractometer with CuKα radiation), scanning electron microscopy (SEM, JEOL 5510), transmission electron microscopy (TEM, JEOL 2100) and X-ray photoelectron spectroscopy (XPS, Escalab Mk II VG Scientific spectrometer with an Al anode). The thermal behavior of pure AP and β-$Ni(OH)_2$-loaded samples was studied by TG (TA-SDT 600) and DSC (Perkin-Elmer DSC7) in N_2 atmosphere. AP was intermixed with β-$Ni(OH)_2$ by grinding in the presence of absolute ethanol in a mortar and dried at 60ºC. Three samples denoted as AP/β-$Ni(OH)_2$-*X*, where *X* = 1, 3 and 5 indicates the weight percentage of β-$Ni(OH)_2$ in the sample, have been prepared.

RESULTS AND DISCUSSION

The XRD pattern of the as-prepared sample, Fig. 1(a), shows peaks that can be easily indexed to the pure hexagonal β-$Ni(OH)_2$ (JCPDS 14-0117). Fig. 1(b) displays the XPS survey scan of the sample. Only signals, corresponding to Ni, O and adventitious carbon are observed. Furthermore, high resolution Ni 2p and O 1s core-level XPS spectra are presented in Fig. 1(c) and Fig. 1(d), respectively. Ni 2p3/2 and Ni 2p1/2 doublet peaks centered at 855.5 eV and 873.1 eV indicate the

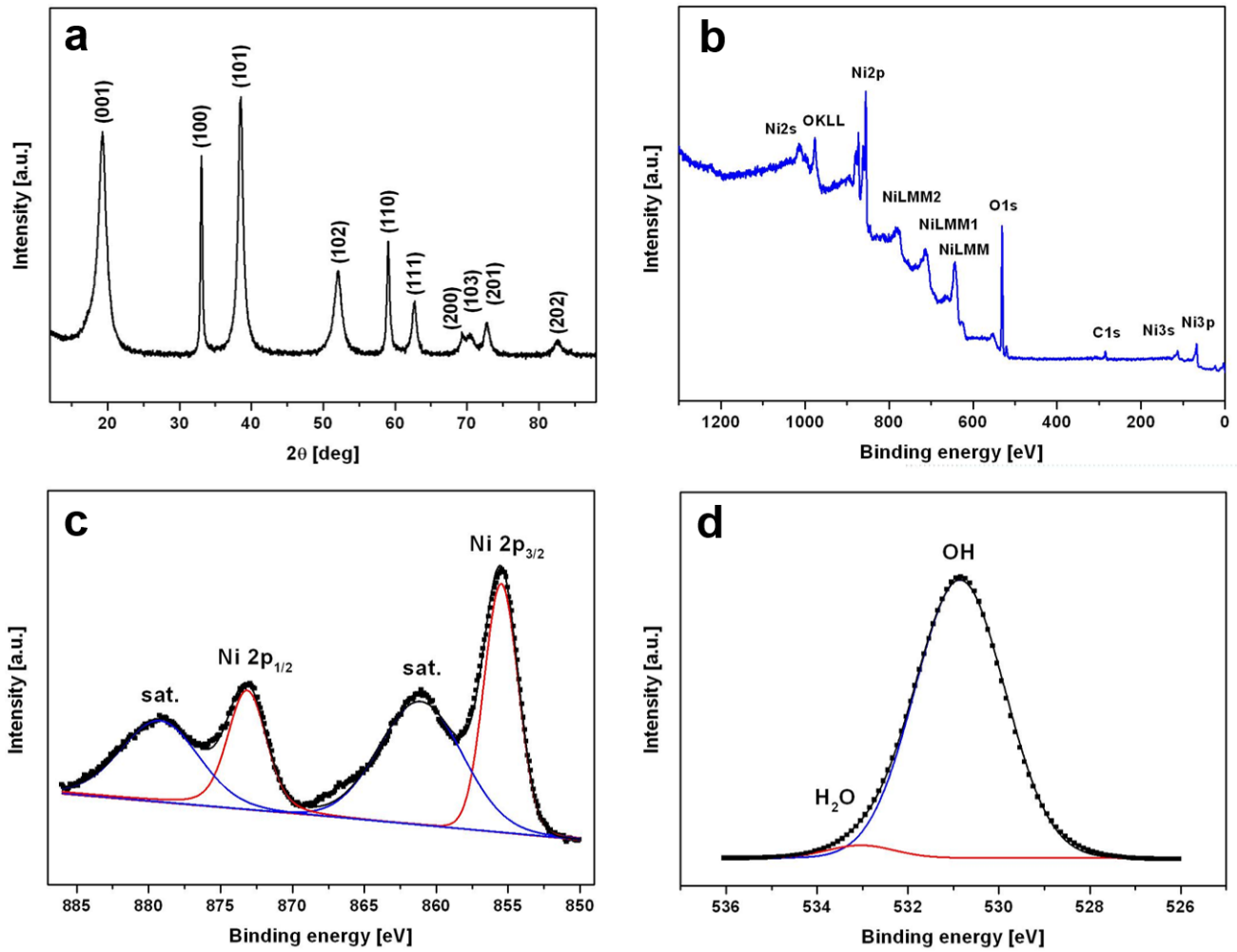

Fig. 1. (a) XRD pattern, (b) XPS survey scan, (c) Ni 2p high-resolution XPS and (d) O 1s high-resolution XPS spectra of the as-prepared β-$Ni(OH)_2$.

presence of Ni^{2+} and perfectly match the reported values for pure $Ni(OH)_2$ [6]. In addition, the deconvoluted O1s peak shows two components at 530.9 and 532.9 eV, which can be assigned to OH- and physically adsorbed H_2O, respectively.

The SEM images of β-$Ni(OH)_2$ are presented in Fig. 2(a) and Fig. 2(b) and reveal submicron spherical particles with morphology that can be associated with the shape of "sand-roses". As can be seen in Fig. 2(b), these microspheres are hierarchically constructed with nanoplates. According to the TEM images (Fig. 2(c) and Fig. 2(d)) the thickness of these interconnected nanoplates varies from 5 to 25 nm. A HR-TEM image is displayed as an insert in Fig. 2(d) and, as shown, the lattice spacing of 0.23 nm can be assigned to the (111) crystal plane of β-$Ni(OH)_2$. The EDS analysis displayed in Fig. 2(e) confirms that the sand-roses are composed of Ni and O, homogeneously distributed throughout the nanoarchitectures.

The exciting morphology of the as-obtained microspheres could be explained by the nucleation and 3D growth of the $Ni(OH)_2$ crystals in the reaction system. As described earlier, during the underwater Leidenfrost process, a fast increase in the concentration of OH^- at

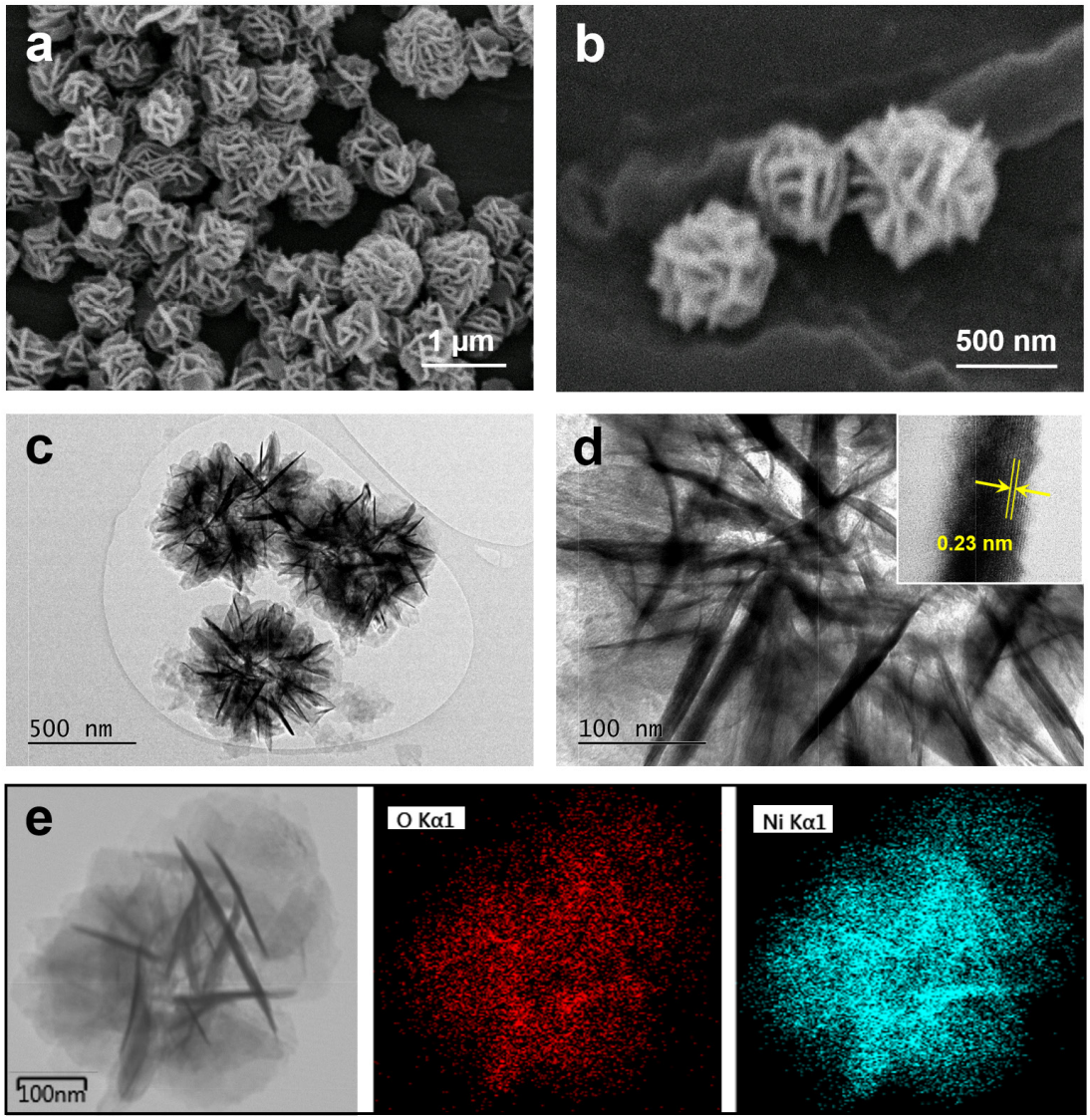

Fig. 2. (a, b) SEM and (c, d) TEM images of β-$Ni(OH)_2$ sand-roses. (e) Element mapping images for Ni and O. The insert of (d) shows HR-TEM lattice image of a nanoplate.

the lowermost region of the solution arises [7]. The latter results in the reaction between $[Ni(NH_3)_6]^{2+}$ and OH^-, yielding $Ni(OH)_2$ and gaseous ammonia. Further, the as-formed hydroxide nanoclusters erupt into colder section of the beaker, where they assemble and grow. The chemical equation is given below.

$$[Ni(NH_3)_6]^{2+} + 2OH^- \rightarrow Ni(OH)_2 + 6NH_3 \quad (1)$$

TG curves (10ºC min^{-1}) of AP and AP/β-$Ni(OH)_2$-*X* are plotted in Fig. 3(a). The decrease in the decomposition temperature of AP in the presence of β-$Ni(OH)_2$ is evident, and it is greater as the amount of hydroxide increases. In the DSC scan (10ºC min^{-1}) of AP, shown in Fig. 3(b), the endothermic peak at 240ºC indicates the transition from the orthorhombic to the cubic polymorphic phase [8]. The exothermic peak at 317.8ºC (low-temperature decomposition reaction, LTD) is due to its incomplete decomposition to NH_3 and $HClO_4$, while the second exothermic peak at 441.4ºC (high-temperature decomposition, HTD) indicates the complete decomposition of AP [8]. As can be seen, the addition of β-$Ni(OH)_2$ has no effect on the endothermic peak of AP, whereas the temperature of the LTD stage is slightly lowered and that of the HTD stage decreases significantly with increasing β-$Ni(OH)_2$ loading. According to Fig. 3(b), the addition of 5 wt. % β-$Ni(OH)_2$ to AP leads to exothermic peaks for LTD and HTD at 302.5ºC and 372.9ºC, respectively. At the same time, β-$Ni(OH)_2$ addition results in an increase in heat release. Compared with 1020 ± 65 J g^{-1} of pure AP, the exothermic value jumps to 1950 ± 160 J g^{-1} for

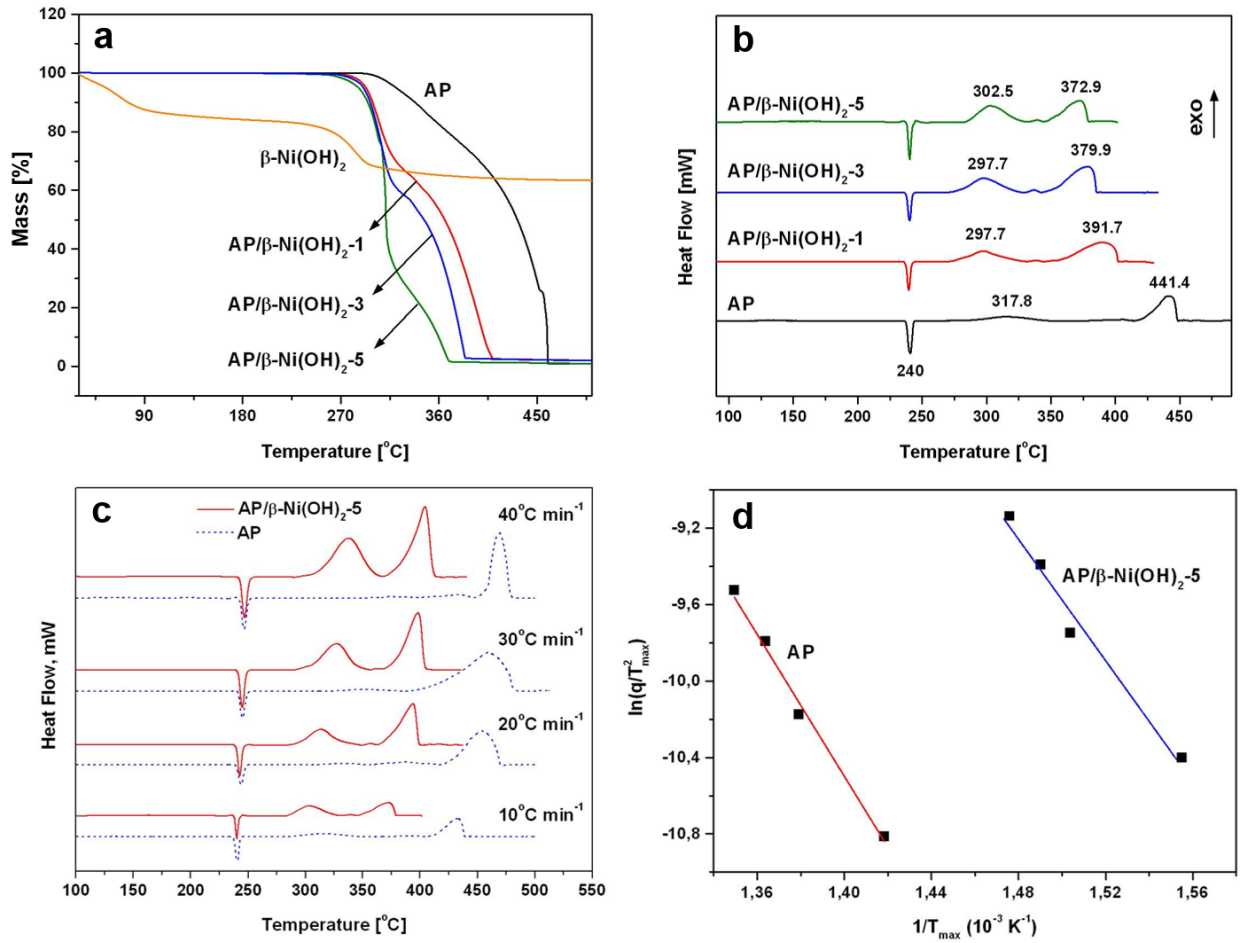

Fig. 3. (a) TG and (b) DSC scans of indicated samples. (c) DSC scans of AP and AP/β-$Ni(OH)_2$-5 at different heating rates and (d) the corresponding Kissinger's plots.

AP/β-Ni(OH)$_2$-1 and shows no further increase at higher β-Ni(OH)$_2$ loadings.

To further determine the accelerating effect of β-Ni(OH)$_2$ microspheres, the thermal decomposition of AP and AP/β-Ni(OH)$_2$-5 was carried out at different heating rates (see Fig. 3(c)). The results of these experiments enable to conduct Kissinger analysis according to the equation [9]:

$$\ln(\beta/T_{max}^2) = \ln(AR/E_a^2) - E_a/RT_{max} \quad (2)$$

where β is the heating rate, T_{max} is the temperature of the DSC HTD peak maximum, A is the pre-exponential factor, R is the universal gas constant, and E_a is the activation energy of the reaction. From the well linearized data of the T_{max} dependence on heating rate, represented in Kissinger coordinates (Fig. 3(d)), the E_a of decomposition for AP was determined to be 126.0 ± 21.0 kJ mol^{-1}, while for AP/β-Ni(OH)$_2$-5 it is equal to 93.0 ± 13.0 kJ mol^{-1}. Again, the strong influence of β-Ni(OH)$_2$ on the decomposition of AP is confirmed by the highly reduced activation energy of the AP decomposition process.

An important question concerns the possible mechanism for the enhanced combustion performance of AP in the presence of β-Ni(OH)$_2$. As illustrated in Fig. 3(a), the TG trace of the as-fabricated β-Ni(OH)$_2$ exhibits two reaction phases. Below ~250ºC a release of the adsorbed water occurs, whereas the dehydration of the majority of the β-Ni(OH)$_2$ to NiO takes place between 250ºC and 350ºC [10]. Thus, it is clear that newly formed NiO species appeared in the reaction mixture during AP/β-Ni(OH)$_2$-*X* thermolysis. To confirm this, we stopped two DSC runs of AP/β-Ni(OH)$_2$-5 at 275ºC and 350ºC, the collected products were washed with water to dissolve AP and the residues were subjected to XRD analysis (Fig. 4). Indeed, the XRD trace of the sample heated to 275ºC shows characteristic peaks of both β-Ni(OH)$_2$ and NiO (JCPDS 47-1049), while at 350ºC only the presence of NiO is detected. In addition, the SEM images depicted in Fig. 4 demonstrate the gradual decay of the initial β-Ni(OH)$_2$ sand-roses. Namely, at 275ºC densification of the crystalline nanoplates is observed, while at 350ºC the spherical shape of the particles is lost and the nanoplates transform into worm-like nanostructures of NiO. On the basis of this outcome, a potential mechanism can be proposed as follows. First, when the AP/β-Ni(OH)$_2$-*X* samples are heated to temperatures above ~250ºC, the β-Ni(OH)$_2$ sand-roses

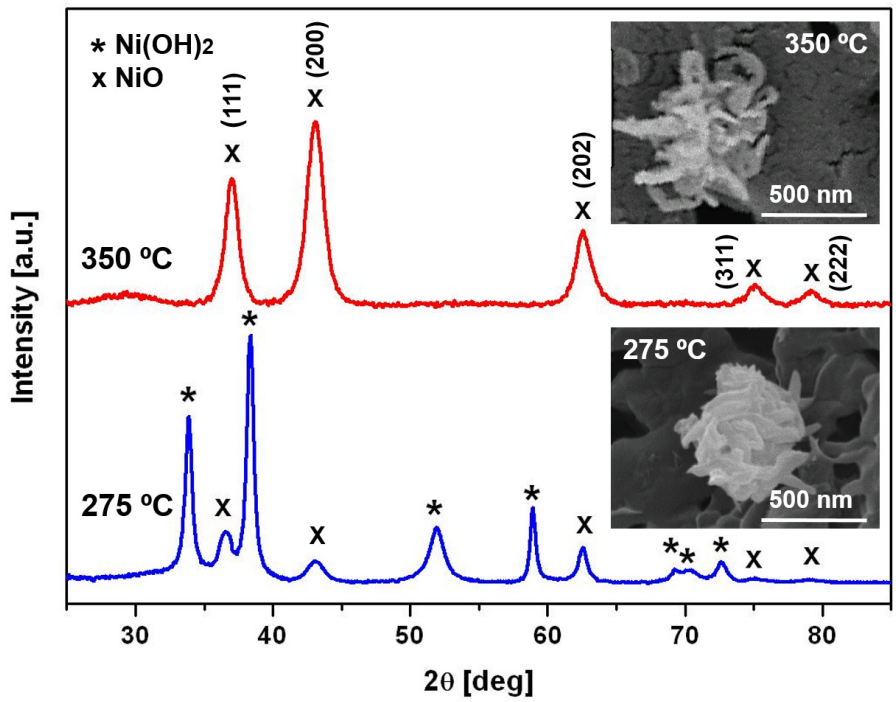

Fig. 4. XRD patterns and SEM images from AP/β-Ni(OH)$_2$-5, heated to 275ºC and 350ºC, respectively, and consequently rinsed with water.

continuously transform into NiO, which serves as a catalyst for the AP thermal decomposition. As previously found, according to the electron transfer theory the active d shell of Ni^{2+} ($3d^8$) on the surface of NiO can speed up electron transfer between the adsorbed NH_4^+ and ClO_4^- species, thereby accelerating the decomposition of AP to molecules such as O_2, N_2O, Cl_2, NO and H_2O [11, 12].

CONCLUSIONS

In summary, we have fabricated novel hierarchically structured β-$Ni(OH)_2$ in the form of sand-roses by a fast and simple solution process. Our experimental results have shown that the fabricated material intensively accelerates the thermal decomposition of AP. β-$Ni(OH)_2$ sand-roses can lower the decomposition temperature of AP by 68.5ºC, increasing the heat release by 91.2 %, while reducing the activation energy to 93.0 ± 13.0 kJ mol^{-1}. It was found that the NiO nanostructures formed in-situ are important factor to drive the catalytic process of AP decomposition. These results provide new insights into the thermal behavior of AP in the presence of nanostructured hydroxides.

Acknowledgements

This study is financed by the European Union-NextGenerationEU, through the National Recovery and Resilience Plan of the Republic of Bulgaria, project No BG-RRP-2.004-0008 and was supported by the European Regional Development Fund within the Operational Programme "Science and Education for Smart Growth 2014–2020" under the Project CoE "National Center of Mechatronics and Clean Technologies" (BG05M2OP001-1.001-0008).

REFERENCES

1. J.P. Agrawal, High energy materials: propellants, explosives and pyrotechnics, Wiley-VCH, Weinheim, 2010.
2. H. Zhai, P. Xu, Y. Li, P. Ye, R. Wang, C. Guo, G. Yang, Improving safety and thermal decomposition performance by the in situ synthesis of core-shell structured ammonium perchlorate/cobalt acetate hydroxide composites, Inorg. Chem. Front., 8, 2021, 2416-2425.
3. H. Zhang, P. Li, W. Cui, C. Liu, S. Wang, S. Zheng, Synthesis of nanostructured γ-AlOOH and its accelerating behavior on the thermal decomposition of AP, RSC Adv., 6, 2016, 27235.
4. G. Tzvetkov, M. Tsvetkov, T. Spassov, Hierarchical CuO microparticles constructed via underwater Leidenfrost process and their Fenton-like catalytic activity, Matter. Lett., 272, 2020, 127840.
5. G. Tzvetkov, M. Tsvetkov, T. Spassov, Facile preparation of edelweiss-like ZnO microparticles with strong UV-violet emission, Vacuum, 192, 2021 110457.
6. M.C. Biesinger, L.W.M. Lau, A.R. Gerson, R.St.C. Smart, The role of the Auger parameter in XPS studies of nickel metal, halides and oxides, Phys. Chem. Chem. Phys., 14, 2012, 2434-2442.
7. M. Elbahri, R. Abdelaziz, D. Disci-Zayed, S. Homaeigohar, J. Sosna, D. Adam, L. Kienle, T. Dankwort, M. Abdelaziz, Underwater Leidenfrost nanochemistry for creation of size tailored zinc peroxide cancer nanotherapeutics, Nat. Commun., 8, 2017, 15319.
8. V. Boldyrev, Thermal decomposition of ammonium perchlorate, Thermochima Acta, 443, 2006, 1-36.
9. H.E. Kissinger, Reaction kinetics in differential thermal analysis, Anal. Chem., 29, 1957, 1702-1706.
10. C.S. Carney, R.E. Chinn, Ö.N. Doğan, M.C. Gao, Isothermal decomposition kinetics of nickel (II) hydroxide powder, J. Alloys Comp., 644, 2015, 968-974.
11. N.M. Juibari, A. Eslami, Synthesis of nickel oxide nanorods by Aloe vera leaf extract: Study of its electrochemical properties and catalytic effect on the thermal decomposition of ammonium perchlorate, J. Therm. Anal. Calorim., 136, 2019, 913-923.
12. S.M. Jebraeil, A. Eslami, Hydrothermal synthesis of graphene oxide/NiO and its influence on the thermal decomposition of ammonium perchlorate, Ind. J. Chem., 61, 2022, 278-284.